

AN EXPERIMENTAL STUDY OF WING PASSAGE FLOWS OF A MICRO WIND TURBINE SYSTEM

M. Zakir Hossain¹, Hiroyuki Hirahara², M. Mahbubul Alam³, Masaaki Kawahashi²
and Yoshitami Nonomura⁴

¹Graduate School of Science and Engineering, Saitama University, Shimo-Okubo-255,
Sakura, Saitama, 338-8570, Japan

²Faculty of Engineering, Saitama University

³Mechanical Engineering Department, Bangladesh University of Engineering & Technology,
Dhaka-1000, Bangladesh

⁴Fujita Co., Ltd., Atsugi, Kanagawa

ABSTRACT

A micro wind turbine system was introduced and its performance was reported in this paper. This system has its wide applicability in remote locations specially in developing countries where there is no grid connected electricity. The main advantage of it is that the system does not need heavy foundation and therefore does not need huge investment. The relations between the energy output, turbine speed, power coefficient, and torque of turbine were reported for the various flow conditions. The details of the flow around the micro wind turbine and the influence of the turbulence were investigated with a particle image velocimetry (PIV). The experimental results show that, the stream passing the spinner approaches towards the blade tip and was accelerated because of exclusive effect of approaching flow due to having a large spinner. Therefore, the flow near the blade tip was fairly increased so that the velocity increase might result in the improvement of the power coefficient. Furthermore, the turbulence of flow passing the blade was analyzed carefully with PIV data. The tip vortex and the vorticity of the flow around the blade were discussed in detail.

Keywords: Micro wind turbine, Power coefficient, Flow measurement, WERM Project for Bangladesh PIV, Tip vortex.

1. INTRODUCTION

In recent years, the interest in wind energy has been growing and several attempt have been developed to introduce cost-effective, reliable wind energy conversion systems all over the world [1]-[4]. A lot of windmills had been introduced and examined its performance practically in developing areas where people do not yet have access to conventional electricity. The large, medium and small windmills have worked commercially for the proper purposes respectively. Many researchers have developed the comparatively large-scale windmill, so they have already applied to many places. On the other hand, although a small windmill would be applied to the area where a large-scale windmill could not be constructed, it has not been developed yet. Because of compactness, portability, simple structure, low noise level in driving, micro wind turbine systems can be used as cluster for various areas, e.g. in urban areas, in a designated construction areas or in monuments etc. Due to their limited space requirement, these systems could also be installed simultaneously with the wind energy resource assessment [5] studies.

We developed a unique micro wind turbine unit and

its integration system for last few years. Testing a several types of windmills, we completed the basic design and proceeded to mass production. In this paper, the relations between the electric output, turbine speed, power coefficient, and torque of turbine were reported for various flow conditions. Then, in order to examine the performance, the details of flow field around the turbines and the influence of the turbulence was investigated with a particle image velocimetry (PIV) in an environmental wind tunnel of 1.8x3.0m². Furthermore, the turbulence of flow passing the blade was analysed with PIV data to discuss the tip vortex and the vorticity of the flow around the blade. Some units were also supplied to the Mechanical Engineering Department of Bangladesh University of Engineering & Technology (BUET), where the scope of integrated research with these micro wind turbines were found most suitable with the ongoing Wind Energy Resource Mapping (WERM) Project for Bangladesh.

2. CONCEPT AND SPECIFICATIONS OF μ F500

The standard of classification of wind turbines was regulated in IEC 61400[5] for large, medium and small

turbines. Although there are many variation in especially small wind turbines, we have no strict regulation in very small wind turbine. By the extension of large or medium size wind turbine, the concept of the general small wind turbine can be explained well. However, the very small wind turbine has fairly variant features in the performance, portability, or application. According to the Gipe [3], we will refer the very small size wind turbine whose diameter is less than 1.25 meters as 'micro wind turbine'. The micro wind turbine unit designed by our project has 500mm diameter and 5kg weight. Hereafter, we will refer the turbine as μ F500 in this paper. The basic specification of μ F500 is as follows.

Table 1 Basic specifications of μ F500

Rotor		
Rotor axis		Horizontal
Basis aerofoil		NACA2404
Number of blades	N	4
Tip diameter	D_T	500mm
Root diameter,	D_R	170mm
Pitch angle of blade		Linear Twisted 18 degrees
Material		Polycarbonate
Tip chord length	C_T	150mm
Root chord length	C_R	96mm
Blade length	L	165mm
Maximum thickness	t_{min}	3.5mm
Tip pitch angle	β_T	80 degrees
Control Design		
Cut in wind speed		4m/s
Rated wind speed		12m/s
Rated rotor speed		1000rpm
Survival wind speed		60m/s
Generator		
Type		Synchronous 16 pole 3 phase
Transmission		Gearless



Fig.1 A view of μ F500

direct drive

3. PERFORMANCE OF μ F500

To evaluate the driving performance of μ F500, an experiment was carried out with an environmental wind tunnel of $3 \times 1.8 \text{m}^2$ of cross section in the range of free stream velocity from 4m/s to 23m/s and for the electric load from 1Ω to 300Ω . The wind tunnel is closed type basically, but the blow down operation is also available depending on the experimental setting. The current experiment was conducted with the closed type setting. The pressure in the measuring section was adjusted to be

equal to the atmospheric pressure, but the blockage effect should not be eliminated from the experimental results completely. However, the micro wind turbine would be driven in the larger turbulence scale than that of itself, so the practical condition should be approximated with the closed loop condition of the wind tunnel.

Wind speed was measured with Pitot tube. Torque of the rotor shaft was measured using a torque meter (Ono Sokki TS-2100). The Power of three phase AC output and DC power after regulating with a rectifier was measured by power tester (Hioki Power Hitester 1301).

Output power of the turbine unit for the various wind speed is shown as a driving parameter of the electric load in Fig.2. The wind turbine started the driving at 3.6m/s and the data was acquired from 4m/s to 23m/s. The electric load resistance was changed from 1Ω to 300Ω . The resistance was controlled to be constant at any measuring condition by using an automatic electric load controller (Kikusui PLZ303WH). In the practical circuits, the impedance of battery is low, so the driving at low resistance is important practically. As the resistance decreases, the torque to rotate the generator increases. Therefore, when the load resistance is low, a large torque is required to rotate the generator. In this situation, the turbine speed is lower than that in the case of higher resistance. The efficiency of the wing deviates from the optimum design point. On the other hand, when the circuit is open, that is, the resistance is an infinite value, the generator rotates with the smallest torque. In this condition, the turbine speed is fastest. Thus, the power coefficient has a maximum between these extreme conditions. In the present case, the optimum electric load might be from 20Ω to 50Ω , consequently.

Figure 3 shows the relation between the torque and turbine speed. The experimental result was rearranged for the wind speed and electric load. When the load resistance is higher than 20Ω , the torque is proportional to the turbine speed approximately. Contrary to this condition, when the electric load resistance is less than 20Ω , the torque curve has a maximum. In this driving condition, the output power is small as shown in Fig.2.

The power output curve for a system consisted of a rotor and generator depends not only on the individual efficiency of both components but also how well they are matched. The relationship between the rotor efficiency and the tip speed ratio with Betz limit as shown in Figure 4. In this figure, the relation between the power coefficient, η_p and tip speed ratio, λ for the various value of the electric load is shown. Here, the term of the power coefficient means the ratio of output power of the rotor to the wind energy. As shown in this figure, the optimum tip

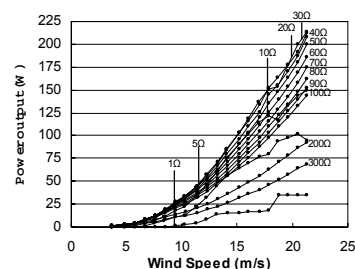


Fig.2 The relation between the power output and free stream wind speed

speed ratio is about 2.9. The maximum power coefficient

the low tip speed ratio. This result is desirable for the

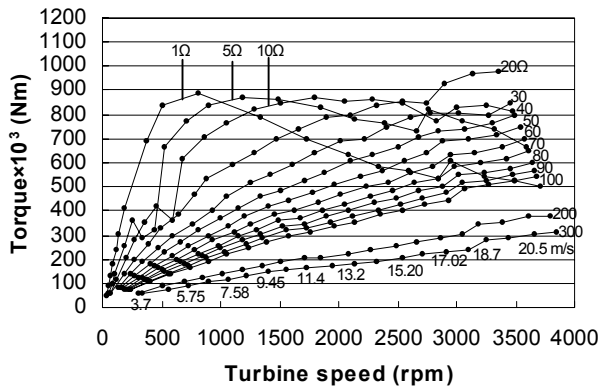


Fig.3 Relation between the Torque and Turbine speed

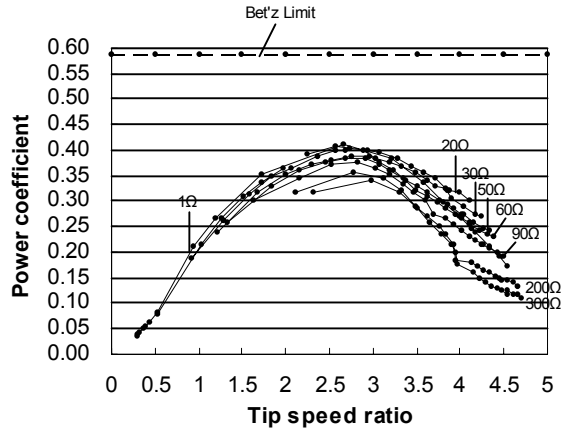
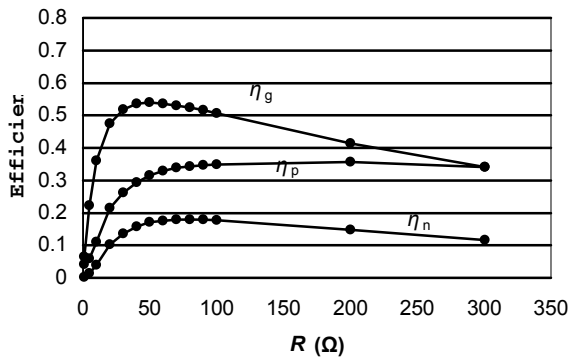
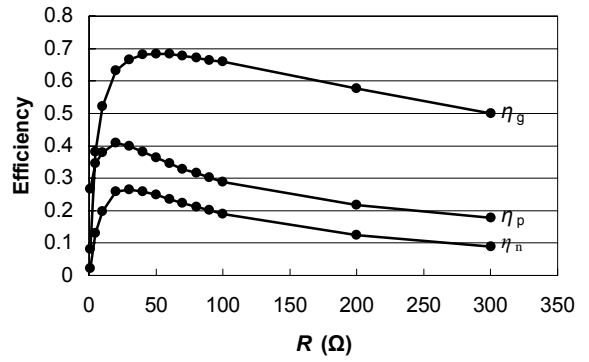


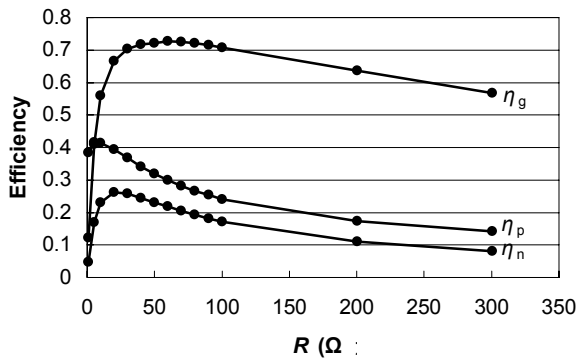
Fig.4 Variation of power coefficient with tip speed ratio.



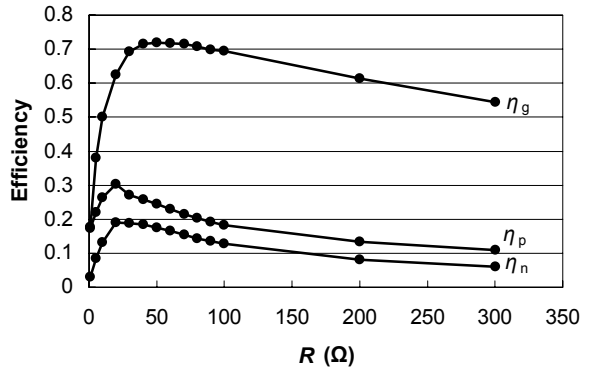
(a) 4.8 m/s



(b) 11.4 m/s



(c) 14.1 m/s



(d) 21.3 m/s

Fig.5 The changes of the coefficients, η_p, η_g, η_n for the output load resistance, R .

is 0.4. This is a desirable value for the wind power system and difficult to establish for the small wind turbine. Especially, since an effective driving in the low turbine speed is the one of the main subjects for $\mu F500$, this result is a most acceptable performance. The fact that $\mu F500$ is well driven at a low tip speed ratio of $2 < \lambda < 3.2$, indicates a good reliability of performance and a driving with lower noise. When $\lambda < 2$, the power coefficient decreases due to the stall of the wing. While $\lambda > 3.2$, the power coefficient decreases due to the induced and viscous drags. Thus $\mu F500$ shows a good performance in

development of micro wind turbine, which might be used in the life space.

As shown in Table.1, one of the features of $\mu F500$ is small aspect ratio. The ratio of rotor radius to tip chord length is 1.67, thus the lift to drag ratio is relatively low. Generally speaking, a wing with small aspect ratio has a good performance in a wide range of attack angle. For the performance of $\mu F500$, it is expected that $\mu F500$ shows a good performance in a wide range of attack angle and good following ability for the wind fluctuation or turbulence.

To demonstrate the influence of free stream velocity and electric load on the energy conversion efficiency, the characteristic curves of the efficiencies are shown in Fig. 5. Here, η_p , η_g and η_n represent the power coefficient, generator conversion efficiency and overall efficiency respectively. The efficiency of rectification by the rectifier unit is also included in generator conversion efficiency and overall efficiency. In this figure, although the abscissa is the electric load which is connected to the output, the change of the electric load is related to the torque change, which is acted on the turbine. So a tolerance for the torque fluctuation is deduced from these curves. When the wind speed is low, e.g. $U_\infty=4.8$ m/s, η_p increases with the load increasing, and is a constant over high resistance. On the other hand, η_g has a maximum at 70Ω . Consequently, the total coefficient has a maximum at 70Ω . When $U_\infty=11.4$, 14.1 , and 21.3 m/s, η_p and η_g has a maximum about 20 or 50Ω , respectively. Then the total efficiency, η_n has a maximum at 30 , 20 and 20Ω , respectively.

4. FLOW VISUALIZATION AND PIV MEASUREMENT

In order to inspect and obtain the detail of flow field around the wind turbine, the flow visualization and velocity measurement is important. Several studies [7]-[11] have been carried out for this sake. We conducted the flow visualization and particle image velocimetry (PIV) measurement in a wind tunnel. Since a wake of the wind turbine is very complicated due to the shedding of the tip vortex and induced flow, particle image velocimetry is most suitable to obtain an instantaneous velocity field and consider the scale of turbulence in the wake.

The outline of the experimental setup is shown in Figure 6. A twin Yag laser was used as a light illumination, which power is 30mJ/pulse. Laser light sheet is parallel to the free stream and introduced through the slit on the top wall of the wind tunnel. The flow images were acquired with a CCD camera (MegaPlus ES1.0), which resolution is 1024x1008 pixels. The distance of the camera position from the light sheet was

490mm. 300 pairs of the flow field was stored in PC for one series of data acquisition. The time separation of the pair images was $100 \mu s$. for all of experimental data. The Yag laser and the optical equipments were mounted on a traversing system for the scanning the test section. By adjusting the lens, the desired thickness and width of the light sheet can be obtained for PIV measurement. The phase locked images were acquired with the signal from the speed counter, which detected the shaft speed, so that the obtained vector field shows the phase locked data with the wing rotation.

An oil smoke generator (Porta smoke generator) has been used to feed the seeding particles with diameter $1\mu m$. The smoke generator was placed at 5m upstream from the test section. Uniform smoke streak was supplied to the main flow after passing the honeycomb and stainless fine grids. The particle density was high enough to record the images. The size of the interrogation was 100×100 mm² or 200×200 mm². The images was analysed by means of a cross correlation calculation. 100×100 vectors were reconstructed from each pair images. The interrogation size in the correlation calculation was 32×32 .

The measurement was carried out at 5 m/s of main stream with 50Ω of electric load. The wind turbine was placed in the uniform flow at centre of the wind tunnel.

he results obtained with PIV measurement is shown in Fig. 7. These vectors show the time mean velocity over 50 pair images. Fig.7 (a) to (c) are velocity vectors and (d) to (f) are the corresponding velocity contours. Figure 7(a) shows the approaching flow near the spinner. $\mu F500$ has a large spinner relative to the turbine diameter. The large spinner was designed to induce accelerated flow around the body. The main stream was decreased due to the body as shown in Fig.7 (a), however, the flow near the blade tip was accelerated due to the exclusive effect by the large body as shown in Fig.7(b). When the mainstream velocity is 5m/s, the velocity near the blade tip increased up to about 6-7m/s approximately. With such low wind speed range, which is available in many locations in Bangladesh, as found from data collected so far [12], this phenomenon could be studied further and substantial results could be achieved.

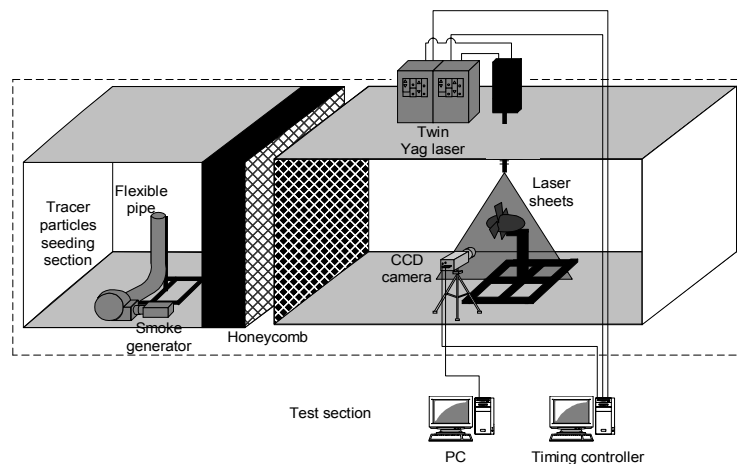


Fig.6 Experimental apparatus with PIV measurement.

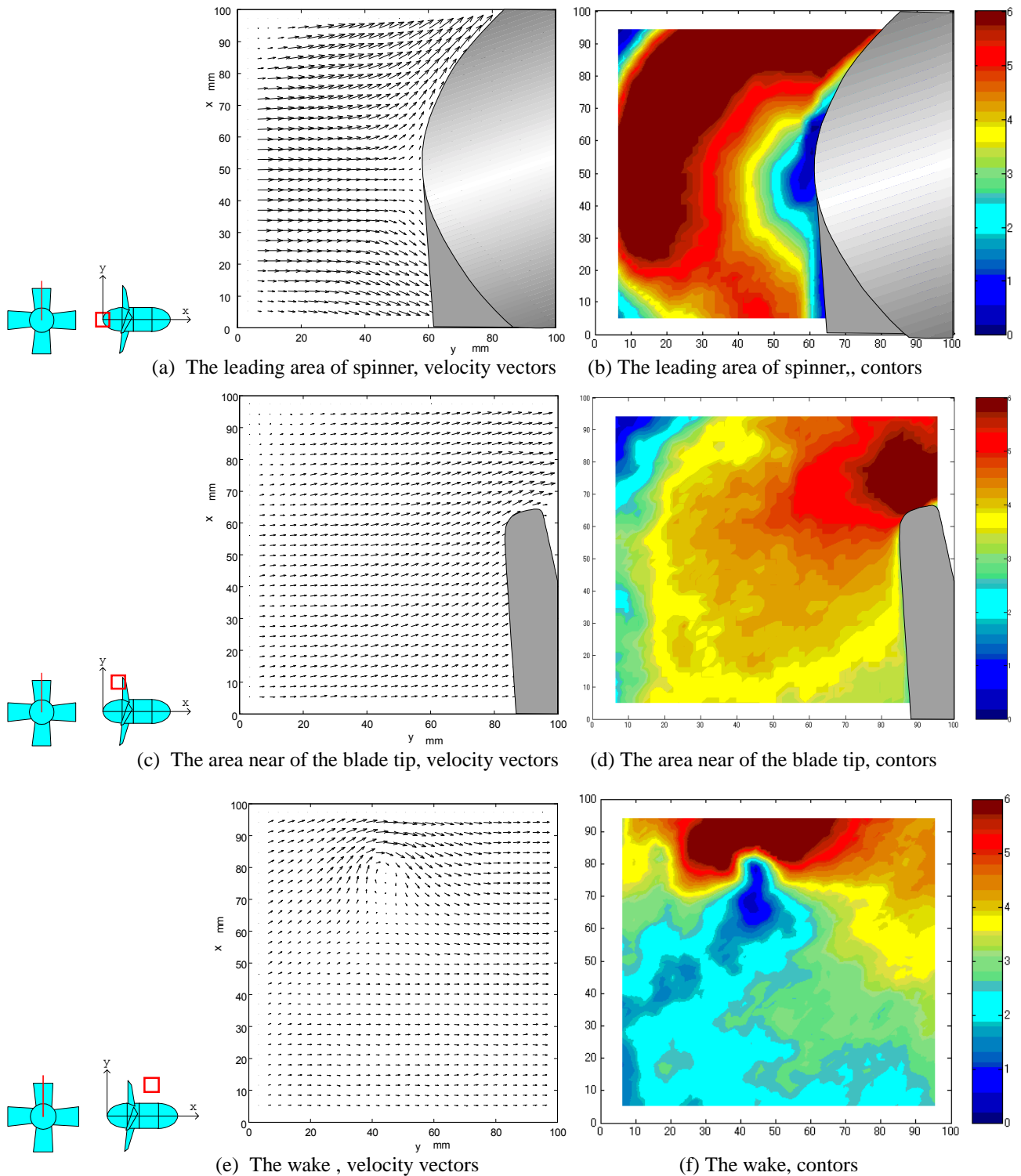


Fig. 7 Velocity vectors and contours at the leading, blade tip and wake regions.

The tip vortex in the wake of blade tip was observed in Fig.7(c) and (f). The wing-tip vortices should be discussed from engineering point of view since these are noise sources and the background of flutter or stall. And also, the tip vortices induced secondary down flow behind the wings. Thus, to investigate the behaviour is very important to optimize the wing design and reduce the noise level. Wind turbines generate noise from multiple mechanical and aerodynamic sources.

Aerodynamic noise originates from the flow of air around the blades. The tip noise depends on the turbulence in the local separated flow region, associated with the formation of the tip vortex. According to Wagner [13], the sound power level can be calculated by using following equation:

$$L_p \approx 50 \log_{10} V_{tip} + 10 \log_{10} r_1 - 1 \quad (1)$$

Calculating the sound level with the above equation, the predicted sound level at the tip of $\mu F500$ becomes 33dB. In the experiment, we cannot detect the discrete sound emission from the wind turbine. On the other hand, the vorticity of tip vortex should be discussed in the system integration of micro wind turbines.

5. CONCLUSIONS

A unique micro wind turbine with 500mm diameter and small aspect ratio was developed for wide use in life space. The performance of the micro wind turbine was tested and investigated the flow around the turbine. The obtained result as follows.

The present micro wind turbine started to produce output power at free stream of 4m/s practically. The optimum load range of output for $\mu F500$ was 20 to 60 Ω . In this range, the power coefficient was 0.4 for the wind speed from 10 to 15m/s. This performance is preferable to introduce as a wind energy resource. The tip speed ratio corresponding to the optimum driving condition was 2.9. Thus $\mu F500$ shows a good performance in the low tip speed ratio. This fact is also strong advantage to introduce this system into the life space or urban space.

The rotational speed was considerably influenced due to the output load in low wind speed region. However, power coefficient is almost constant except for the case of very low resistance. The power coefficient was about 0.36. When the free stream is fast, the power coefficient is sensitive and the optimum driving region is limited in small range of output electric load. As wind speed increased, the power coefficient decreased due to the induced and viscous drag.

Conducting the flow visualization and PIV measurement around the wind turbine, it was confirmed that the free stream was accelerated as approaching the blade tip, so that the turbine has a geometrical advantage in the meaning of the design concept. Tip vortex shed from the blade tip was also visualized clearly. Obtained vorticity will be available to use in the analysis of the wake of a integrated micro wind turbine system.

6. REFERENCES

1. Celik, A. N., 2003, "Energy Output Estimation for Small-Scale Wind Power Generators Using Weibull-Representative Wind Data", J. Wind. Eng. Aerodyn., 91:693-707
2. Hopkins, W., 1999, "Small to medium size wind turbines; Local use of a local resource", Renewable Energy, 16,944-947
3. Gipe, P., 1999, "Wind Energy Basics", Chelsea Green Publishing Company, Vermont, Totnes, England.
4. Hansen, A. C. and Butterfield, C. P., 1980, "Current Development in Small Wind Energy Conversion Systems", J. of Ind. Aerodyn., 5:337-356.
5. Alam, M.M., 2002, "Wind Energy Resource Mapping (WERM) Project for Bangladesh-the Enviaible Approach for Successful Implementing of Wind Energy Systems". Proc. Of the Training Workshop on RET for Clean Environment and Sustainable Development, Jordan, 32-50.
6. IEC 61400-2, 1996, Wind turbine generator

7. Ebert, P. R., 1997, "The near wake of a model horizontal-axis wind Turbin-1, Experimental arrangements and initial results", Renewable Energy, 12(3): 225-243
8. Grant, I., Mo, M., Pan, X., Parkin, P., Powell, J., Reinecke, H., Shuang, K., Coton, F. and Lee, D., 2000, "An Experimental and Numerical Study of the Vortex Filaments in the Wake of an Operational Horizontal-axis, wind Turbine", J. wind Eng. Aerodyn., 85:177-189
9. Vermeer, L. J., 2001, "A Review of Wind Turbine Wake Research at TUDELFT", AIAA- 2001-0030
10. Johnson, J. and Sørensen, N. N., 2002, "Numerical Investigation of Three Wind Turbine Blade Tips", Risø-R-1353(EN)
11. Afjeh, A. A. and Keith, T. G., 1989, "A simple computational method for performance prediction of tip-controlled horizontal axis wind turbines", J. wind. Eng. Aerodyn., 32:231-245
12. Alam, M.M and Murtaza, M. 2003, "Some Results of Wind Energy Resource Mapping (WERM) Project for Bangladesh and Future Prospects" Proc. Of 3rd Int. Conf. On Renewable Energy for Sustainable Development, IEB, Dhaka, 261-270.
13. Wagner, S. Bareiss, R. and Guidat, G., 1996, "Wind Turbine Noise", springer-Verlag

7. NOMENCLATURE

Symbol	Meaning	Unit
λ	Tip speed ratio	
R	Load resistance	Ω
η_p	Power coefficient	
η_g	Generator conversion efficiency	
η_n	Overall efficiency	
U_∞	Free stream velocity	m/s
L_p	Sound Power level	dB
V_{tip}	Wind turbine tip velocity	m/s
r_1	Wind turbine tip radius	m